Catalysis Today 152 (2010) 78–87

Contents lists available at ScienceDirect

Catalysis Today

journal homepage: www.elsevier.com/locate/cattod

Theoretical investigation of ethane dehydrogenation on cationic Zn species in ZSM-5 zeolites—The second Al center in vicinity of the cation is essential for the accomplishment of the complete catalytic cycle

Hristiyan A. Aleksandrov, Georgi N. Vayssilov *

Faculty of Chemistry, University of Sofia, Blvd. J. Bauchier 1, 1126 Sofia, Bulgaria

ARTICLE INFO

Article history:
Available online 12 February 2010

Keywords:
Zeolite
Alkane dehydrogenation
Zinc
Entropy
Free energy
Paired Al sites

ABSTRACT

Ethane dehydrogenation on Zn,H-ZSM-5 was modeled by density functional calculations on isolated zeolite fragment. Three types of cationic Zn species, that are assumed to exist in the samples prepared by ion exchange, were considered as active sites for the process: Zn^{2+} in the vicinity of paired Al centers as well as $ZnOH^+$ and ZnH^+ in the vicinity of one isolated Al site. For all modeled mechanisms and active sites we accounted for the influence of the entropy. The results suggest that the process on Zn^{2+} cation at paired Al site has the lowest free energy of activation. The calculations also highlight the essential role of the second Al center in vicinity of the zinc cation for the reaction since it generates basic framework oxygen center participating in the reaction steps with lowest activation barrier. In absence of a second Al center close to the zinc species (as in the models with isolated Al sites) the reaction is blocked due to formation of rather stable intermediates ZnH^+ or $Zn(C_2H_5)^+$ that cannot be decomposed due to the too high activation barriers on the next stages of the dehydrogenation process.

1. Introduction

One of the perspective catalysts for the transformation of light alkanes in more valuable products as alkenes, aromatic compounds and hydrogen is Zn,H-ZSM-5 zeolite [1–8]. The extensive experimental [2,7,9–11] studies of these zeolites have suggested that depending on the method for preparation of the samples several types of Zn-containing cationic species might exist and/or act as active sites for dehydrogenation of ethane or propane. Due to its +2 positive charge, the bare Zn^{2+} cation is accommodated typically in vicinity of the parts of zeolite framework containing two closely located Al centers and in this way the local electroneutrality of the zeolite system is preserved. In addition to these regular zinc cationic sites located at Al pairs, Zn^{2+} cations are suggested to exists as "partially compensated species" in vicinity of isolated Al sites and far from the second Al center which virtually accomplishes the charge compensation for the whole zeolite framework. Such type of sites is proposed to exist when the Zn,H-ZSM-5 sample is prepared by exchange of H-ZSM-5 zeolite with Zn vapors [10,12–14]. Other proposed types are $ZnOH^+$ [9] and $ZnOZn^{2+}$ [15–19] species. While confirming the existence of the former type of species, presumably in vicinity of isolated Al sites, Iglesia and co-workers discarded the latter species in samples prepared by ion exchange on the base EXAFS investigation [2]. Such $ZnOZn^{2+}$ species is confirmed to exist only when Zn,H-ZSM-5 is prepared by incipient wetness impregnation [2,15–17,19]. We have recently modeled computationally four different types of cationic Zn species, Zn^{2+}, $ZnOH^+$, $Zn(H_2O)^{2+}$ and $ZnOZn^{2+}$, coordinated to fragments of ZSM-5 zeolite [20–23] and found that at zeolite fragments containing two Al centers the most stable Zn species are $Zn(H_2O)^{2+}$. In such position the $ZnOH^+$ species are unstable since they spontaneously attract the zeolite proton from the neighboring bridging OH group, which compensates the charge of the second Al atom in the zeolite fragment, and form $Zn(H_2O)^{2+}$easily. By this reason $ZnOH^+$ species in Zn,H-ZSM-5 zeolites can exist only in vicinity of isolated Al sites, in agreement with previous experimental hypothesis [2]. On the other hand, several computational studies [20,21,24,25] suggested that $ZnOZn^{2+}$ species are considerably less stable compared to the other cationic Zn-containing species in zeolite.

Experimentally, the dehydrogenation of light alkanes was found to occur on Zn,H-ZSM-5 samples prepared by ion exchange [1,4,6–8], impregnation [5,7], and Zn vapor deposition [4,5]. According to Iglesia and co-workers, the role of Zn species in the catalytic process is facilitation of the recombination and desorption of H_2 from the catalytic site [1,3]. By IR spectroscopy Kazansky and Pidko [12] established formation of ethanide $Zn(C_2H_5)^+$ species and restoration of bridging OH groups after heating the sample

* Corresponding author.
E-mail address: gnv@chem.uni-sofia.bg (G.N. Vayssilov).

0920-5861/$ – see front matter © 2010 Elsevier B.V. All rights reserved.
doi:10.1016/j.cattod.2010.01.001

with ethane adsorbed on Zn,H-ZSM-5 prepared by Zn vapor deposition.

There are also several computational studies of the reaction mechanism. In an early investigation, Frash and van Santen [26] modeled ethane dehydrogenation on Zn^{2+} located at four-membered ring and showed that the dissociation of the ethane molecule to carbanion $C_2H_5^-$ and H^+ is energetically more favorable compared to the alternative carbenium mechanism via dissociation to $C_2H_5^+$ and H^-. Zhidomirov et al. [27] considered the process on Zn^{2+}, located close to only one Al center in a five-membered zeolite ring, while a second Al center is positioned in the neighboring ring. The reaction intermediate $Zn(C_2H_5)^+$ in this case is rather stable, −135 kJ/mol, since H^+ released from ethane dissociation compensates the distantly located second Al center. The second stage, β-transfer of hydride anion from the CH_3 group to the Zn center resulting in formation of C_2H_4 and ZnH^+ species has apparent activation barrier (energy of the transition state, calculated with respect to the reactants) of 65 kJ/mol, while the final step – recombination and desorption of H_2, has high apparent activation energy, above 200 kJ/mol [28], since the regeneration of the catalytic site results in formation of one uncompensated Al center.

Recently, Pidko and van Santen modeled ethane dehydrogenation on Zn^{2+} ions, located close to one or two Al centers, as well as on $ZnOZn^{2+}$ species [29]. After the initial heterolytic dissociation of ethane, they suggested alternative way for decomposition of $C_2H_5^-$ into ethene via simultaneous formation of H_2 by a hydride from the methyl group and proton from the bridging OH group of the zeolite produced in the first step of the mechanism. In this way the apparent activation energy for this reaction on Zn^{2+} located close to two Al centers is 222 or 226 kJ/mol, depending on which O center participates in the initial proton abstraction. According to the authors, the apparent activation energy decreases to 153 kJ/mol when the reaction takes place on Zn^{2+} ions located close to only one Al center. The explanation of the catalytic activity of Zn,H-ZSM-5 zeolites on the base only of partially compensated Zn^{2+} species, however, meets two problems:

(i) formation of such centers requires overcoming of rather high electrostatic energy [30,31];
(ii) such species are proposed to exist only when the sample is prepared by treatment with Zn vapor [10,12,13], while the ethane dehydrogenation occurs also on Zn,H-ZSM-5 samples prepared by ion exchange or by impregnation (in particular for Si/Al ratios <40), where the zinc-containing ions located close to isolated Al centers are proposed to be monovalence $ZnOH^+$ species.

In the present investigation we modeled the mechanism of ethane dehydrogenation on cationic Zn-containing species located close to isolated and paired Al sites, which could exist in pores of Zn,H-ZSM-5 zeolites prepared by ion-exchange technique. In the case of paired Al centers as active sites we considered bare Zn^{2+} cations produced after desorption of water molecule from the most stable species in such position, $Zn(H_2O)^{2+}$, at the typical reaction temperature, 723–823 K [1,3,7,32]. At isolated Al sites we modeled the reaction on $ZnOH^+$ and ZnH^+; the latter species could be formed during the interaction between $ZnOH^+$ and ethane. In addition to the carbanionic mechanism considered in the previous computational studies [26,27,29], we studied a synchronous mechanism, in which in one step a hydride ion and a proton from ethane are transferred to the Zn^{2+} species and O center of the active site, respectively. In this way the ethene molecule is formed and leaves without adsorption on the catalytic center. At variance from the previous studies, for the transition states of all modeled mechanisms and active sites we considered in details the influence of the entropy, which is crucial for the correct analysis of the preferred mechanism at the high reaction temperature, above 700 K [1,3,7,32]. We have shown that the presence of the second Al center in vicinity of the zinc cation is essential for the reaction since it generates basic oxygen center participating in the reaction steps with lowest activation barrier. In absence of a second Al center close to the zinc species the reaction is blocked due to formation of rather stable intermediates that cannot be decomposed due to the too high activation barriers.

2. Methods and models

Initially, we optimized the MFI structure at the molecular mechanical (MM) level with the program GULP [33], using a previously reported shell model force field (FF) [34,35]. From this structure we choose a model cluster representing five-membered zeolite ring to be treated at the quantum mechanical level. In MFI structure this ring faces the main channel of the structure. The cluster (denoted as zeolite fragment Z2), used for modeling of ethane dehydrogenation on Zn^{2+} species, contains two Al centers, located at the crystallographic positions T2 and T9. The other model cluster (denoted as zeolite fragment Z1), used for modeling of ethane dehydrogenation on $ZnOH^+$ and ZnH^+, has the same structure but contains only one Al center at the position T9.

The dangling bonds were saturated by H atoms, and the direction of these bonds at the cluster boundary was fixed as obtained in the zeolite structure optimized with the MM model. The lengths of the corresponding T–H or O–H bonds were pre-optimized, keeping all other atoms in the cluster fixed, followed by an optimization of the cluster with fixed positions of all saturating H atoms. In the subsequent geometry optimization steps, only the positions of the oxygen centers, the protons of the bridging OH groups, and the guest species were relaxed, while the positions of terminated H atoms and T atoms were fixed.

The calculations were performed with the program Gaussian03W [36] using the gradient-corrected exchange-correlation functional suggested by Becke and Perdew [37] with 6-311+G** type of basis sets for all atoms.

The enthalpies of all investigated species were obtained from the calculated electronic energies corrected for the zero point vibrational energy derived from frequency calculations of the optimized structures; in addition we also took into account the internal thermal energy. The calculated vibrational frequencies are in harmonic approximation, as the force constants of the vibrational modes are obtained analytically. Since part of the system is fixed during the geometry optimization, this leads to appearance of imaginary frequencies (negative force constants). These frequencies were suppressed by removing the contributions of the fixed atoms in the Hessian matrix. All obtained transition states have only one imaginary frequency, which corresponds to the eigenvector, corresponding to the reaction path.

The reported entropy of the reactants, intermediates and transition states includes the contributions of all degrees of freedom for the gas molecules and only vibrational degrees of freedom for the zeolite clusters and the adsorption complexes. The frustrated rotational and translational modes of the guest species were accounted for as a part of the vibrational component of the partition function.

3. Results

As it was described in Section 1, at high temperature the type of the preferred zinc species in the pores of Zn,H-ZSM-5, prepared by ion exchange, depends on the relative location of the Al centers in the framework: at isolated Al center this is $ZnOH^+$ and at two closely located Al centers (e.g. Al pair) this is Zn^{2+}. By this reason we investigated the mechanism of ethane dehydrogenation on two

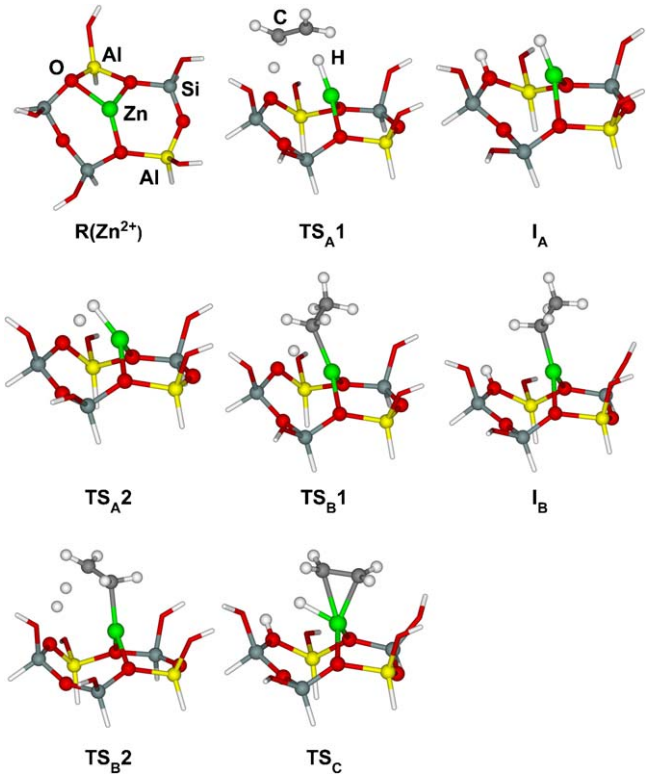

Fig. 1. Structures of transition states and intermediates of the considered mechanisms: A–C, of ethane dehydrogenation on Z2/Zn^{2+}.

cluster models: Z2/Zn^{2+} (Fig. 1), where Zn^{2+} is coordinated to a zeolite fragment containing two Al centers, and Z1/$ZnOH^+$ with $ZnOH^+$ coordinated at a fragment with a single Al center (Fig. 2). During the interaction of ethane with $ZnOH^+$ another type of Zn-containing species, ZnH^+, could be formed and by this reason we modeled the dehydrogenation reaction also on the active site Z1/ZnH^+. Structures of transition states and intermediates for the different mechanisms are shown in Figs. 1 and 2 and selected interatomic distances are reported in Table 1. The calculated values of relative enthalpies ΔH and entropies ΔS of all stationary points

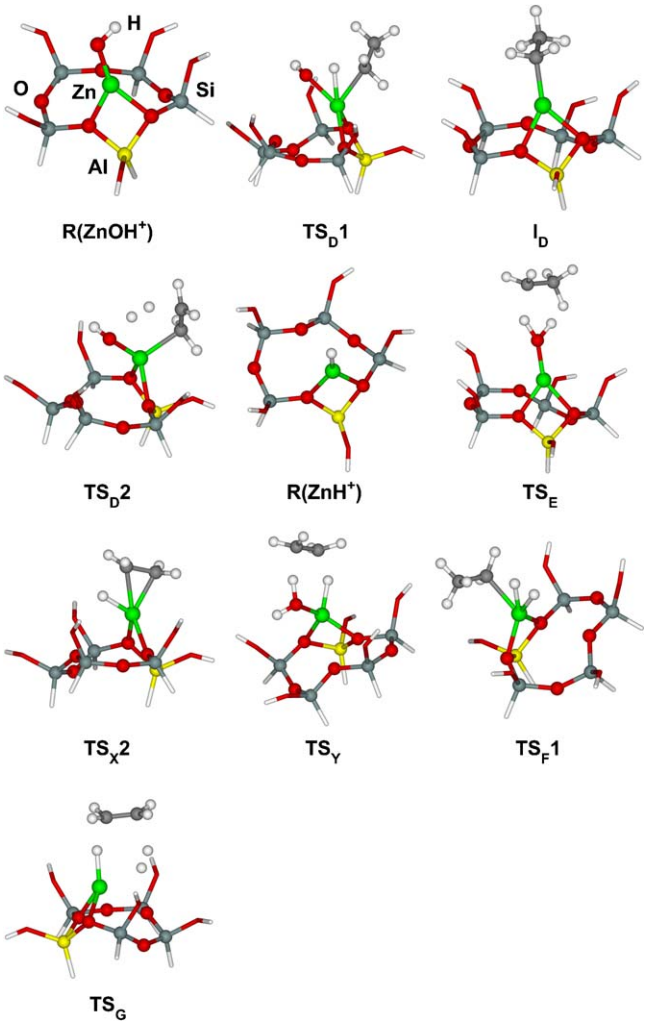

Fig. 2. Structures of the transition states and intermediates in the considered mechanisms: D–G, X, and Y, of ethane dehydrogenation on Z1/$ZnOH^+$.

Table 1
Selected interatomic distances (in pm) in the optimized structures of all considered intermediates, transition states and gas phase molecules C_2H_6, H_2 and C_2H_4.

Structure	O[a]–H	Zn–H	H–H	C–C	C–H	Zn–C
TS_A1	128	157		139	135	
I_A	98	154	402			
TS_A2	130	166	102			
TS_B1	121			154	154	206
I_B	98			154	110	198
TS_B2	157		84	142	153	204
TS_C	98	168		143	162	211, 219
TS_D1	130	178		154	138	220
I_D						196
TS_D2	98, 146		87	141	169	214
TS_E	109, 118		122	149	123, 168	
TS_X2		168		144	166	209, 216
I_E		152				
TS_F1		179, 215	110	154	157	215
TS_Y	113	164		142	148, 161	
TS_G		163, 211	82	138	157, 171	
C_2H_6				154	110	
H_2			75			
C_2H_4				134	109	

[a]For the mechanisms A–C, O atom is from zeolite bridging OH group; in mechanisms D, E and Y, O atom is from $ZnOH^+$.

Table 2
Enthalpy and entropy differences (at 298 K) in the considered intermediate and transition state structures with respect to the corresponding values for (Z2/Zn^{2+} + C_2H_6)[a] for the structures, included in the mechanisms A–C; with respect to (Z1/$ZnOH^+$ + C_2H_6)[b] for the structures in mechanisms D, E, and X, Y; and with respect to (Z1/ZnH^+ + C_2H_6)[c] for the structures in the mechanisms F and G.

Mechanism	Structure	ΔH (kJ/mol)	ΔS (J/mol K)
A[a]	TS_A1	153	−145
	I_A	131	18
	TS_A2	164	−8
B[a]	TS_B1	79	−191
	I_B	76	−128
	TS_B2	154	−152
C[a]	TS_B1	79	−191
	I_B	76	−128
	TS_C	272	−156
	I_A	131	18
	TS_A2	164	−8
D[b]	TS_D1	117	−204
	I_D	49	−12
	TS_D2	215	−206
E[b]	TS_E	277	−198
F[c]	TS_F1	221	−171
	I_D	41	−32
	TS_X2	246	−56
G[c]	TS_G	233	−170
X[b]	TS_D1	117	−204
	I_D	49	−12
	TS_X2	254	−36
	$P(ZnH^+)$	144	138
Y[b]	TS_Y	211	−189
	$P(ZnH^+)$	144	138

are shown in Table 2. They are calculated with respect to the corresponding initial state of the reaction: the active center and ethane molecule. The reported values take into account the gas products (C_2H_4, H_2 or H_2O) released in the previous stages of the process.

3.1. Ethane dehydrogenation on Zn^{2+} species at paired Al site

We considered three mechanisms of ethane dehydrogenation on Zn^{2+} species coordinated to cluster model with two Al centers, which are shown in Fig. 3. In this scheme, the initial active center Z2/Zn^{2+} is denoted as R (reactant at the left hand side), while the same center which is recovered at the end of the catalytic process is denoted P (product at the right hand side). We considered two ways for ethane activation – via the interaction of both or of one of the methyl groups with the active center. In the first case, the synchronous mechanism (denoted as A) occurs via transition state TS_A1 (Fig. 1), in which two H atoms from both methyl groups are transferred simultaneously as a hydride ion and as a proton to the Zn^{2+} and to a basic zeolite O center, respectively. In this stage ethene molecule is directly formed and leaves the reaction site. The remaining intermediate I_A (Fig. 1) represents heterolytically dissociated H_2 at the active site. The second step of this mechanism is H_2 recombination and desorption from the active site, which occurs via transition state TS_A2 (Fig. 1).

The second way for initial activation of ethane on the active site is analogous to the mechanisms reported in the earlier studies [26,27,29] via formation of carbanionic $C_2H_5^-$ species. It starts with heterolytic dissociation of the ethane via transition state TS_B1 (Fig. 1), where one of the C atoms interacts with Zn^{2+} and a H atom from the same methyl group is transferred as a proton to a basic O center from the zeolite. The resulting intermediate I_B (Fig. 1) represents $Zn(C_2H_5)^+$ species and a bridging zeolite hydroxyl group. There are two possibilities for decomposition of this intermediate: (i) formation in one step of ethene and H_2 by H^- from the methyl group of ethanide anion and H^+ from the bridging OH group of the zeolite via TS_B2 (Fig. 1) (denoted as mechanism B); or (ii) by β-transfer of a hydride anion from the methyl group to the zinc center and desorption of ethene via transition state TS_C (Fig. 1) leading to formation of the intermediate I_A, which afterwards releases a molecule H_2 via transition state TS_A2. The last mechanism is denoted C.

The first transition state TS_A1 of the synchronic mechanism A is late, i.e. its enthalpy and structure are closer to the intermediate I_A and the produced ethene (Tables 1 and 2). The second transition

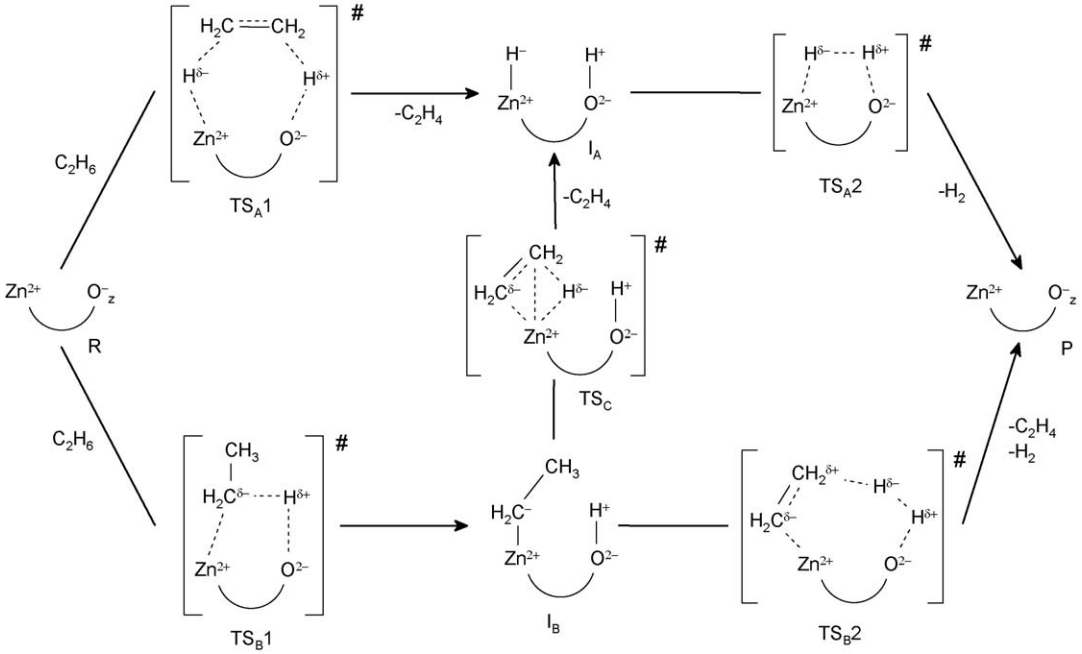

Fig. 3. Mechanisms A (upper path), B (lower path) and C (via the structure in the middle) of ethane dehydrogenation on Zn^{2+} located at Al pair.

state TS_A2 of this mechanism concerns recombination of H_2 from the intermediate. The calculated ΔH values for the two transition states are similar, 153 and 164 kJ/mol. With ΔH of 131 kJ/mol, the intermediate I_A is by only 6 kJ/mol more stable than the product (this difference characterizes the energy gain due to dissociative adsorption of H_2 on the active site $Z2/Zn^{2+}$).

In the carbanionic mechanism B, the first transition state TS_B1, corresponding to heterolytic dissociation of ethane on the active site, is also late (Tables 1 and 2). Similarly, the second transition state in the mechanism B, TS_B2, is structurally closer to the final products of the reaction, ethene and H_2 than to the intermediate I_B. Both TS_B1, with ΔH = 79 kJ/mol, and the intermediate I_B, ΔH = 76 kJ/mol, of the mechanism B are notably more stable than corresponding species obtained in the synchronous mechanism A. The relative enthalpy of the second transition state, TS_B2, ΔH = 154 kJ/mol, is similar to both transition states of the mechanism A, TS_A1 and TS_A2.

Mechanism C includes subsequently TS_B1, I_B, TS_C, I_A and TS_A2. The only transition state that is not included in the mechanisms A and B is TS_C (for β-transfer), which is considerably less stable, ΔH = 272 kJ/mol (Table 2), than the transitions states described above.

3.2. Ethane dehydrogenation on $ZnOH^+$ species at isolated Al sites

On the alternative catalytic species, $ZnOH^+$, located close to an isolated Al center, we considered again the same two ways of activation of C_2H_6 molecule – via interaction of one or both methyl groups with the active center (Fig. 4). The main difference from the previous active site is the absence of additional basic oxygen center from the zeolite fragment in vicinity of the zinc species which in the previous case subtracted a proton from ethane. By this reason, as basic site here we considered the oxygen center from the $ZnOH^+$ species. The first mechanism, denoted as D, includes heterolytic cleavage of a C–H bond towards $C_2H_5^-$ anion coordinated to the zinc cation and H^+ interacting with the O center from the $ZnOH^+$, TS_D1 (Fig. 2). This reaction step should lead to the intermediate $Zn(C_2H_5)(H_2O)^+$ coordinated to the zeolite ring, however during the optimization of this structure the water molecule leaves the active site and intermediate I_D, representing adsorbed $Zn(C_2H_5)^+$ species (Fig. 2), is formed. Due to the desorption of H_2O in the first step, the catalytic center $ZnOH^+$ can be recovered only in presence of water in the gas phase. Thus, the interaction of the intermediate I_D with water via transition state TS_D2 (Fig. 4) leads to formation of ethene and H_2 and restoration of the catalytic center. In the second mechanism, denoted as E, the ethane molecule transfers simultaneously a proton and a hydride ion to the O and H atoms from the hydroxyl group of the $ZnOH^+$ species (Fig. 2). In this way via transition state TS_E the products C_2H_4 and H_2 are formed in a single step and the catalytic center is restored.

In the first transition state of mechanism D, TS_D1, the transferred proton is located close to the zinc cation at Zn–H distance of 178 pm (Table 1). The intermediate I_D, $Zn(C_2H_5)^+$, have similar structure as the intermediate of the mechanism B, I_B; the only difference is that in I_D the species are coordinated to zeolite ring containing isolated Al center, while in I_B, the zeolite fragment contains two Al centers and $Zn(C_2H_5)^+$ is located in the middle of the zeolite ring. In the second transition state TS_D2, the molecule H_2 is formed from H^+ from the water molecule and H^- from the ethanide anion without the participation of Zn^{2+}. This is accompanied by desorption of the formed ethene from the catalytic site.

The relative enthalpy of the transition state TS_D1 is 117 kJ/mol, but ΔH of the second transition state TS_D2, 215 kJ/mol (Table 2), is significantly higher than the values for the rate-limiting steps in the mechanisms A and B described above. To some extend this could be caused by the lower acidity of the proton donor, H_2O compared to the zeolite OH group in mechanism B, and the higher stability of the intermediate I_D compared to the intermediate I_B, by 27 kJ/mol. The latter observation suggests that the ethanide anions are more stable on zinc species located close to isolated Al centers than on those coordinated in vicinity of paired Al sites.

The transition state TS_E for formation of ethene and hydrogen via interaction of ethane with the oxygen and hydrogen atoms from the hydroxyl ligand of the $ZnOH^+$ species is rather unfavorable with ΔH = 277 kJ/mol (Table 2).

3.3. Ethane dehydrogenation on ZnH^+ species at isolated Al sites

We also studied the possibility of formation of alternative catalytic center ZnH^+ (Fig. 5) from $Z1/ZnOH^+$. Such center can be obtained when ethane interacts with $Z1/ZnOH^+$ in absence of water. It also can be formed in presence of partially compensated zinc ions, located close to isolated Al centers in the zeolite lattice, since such Zn species is formed mainly when H-ZSM-5 is treated with Zn vapor at high temperature [10–13].

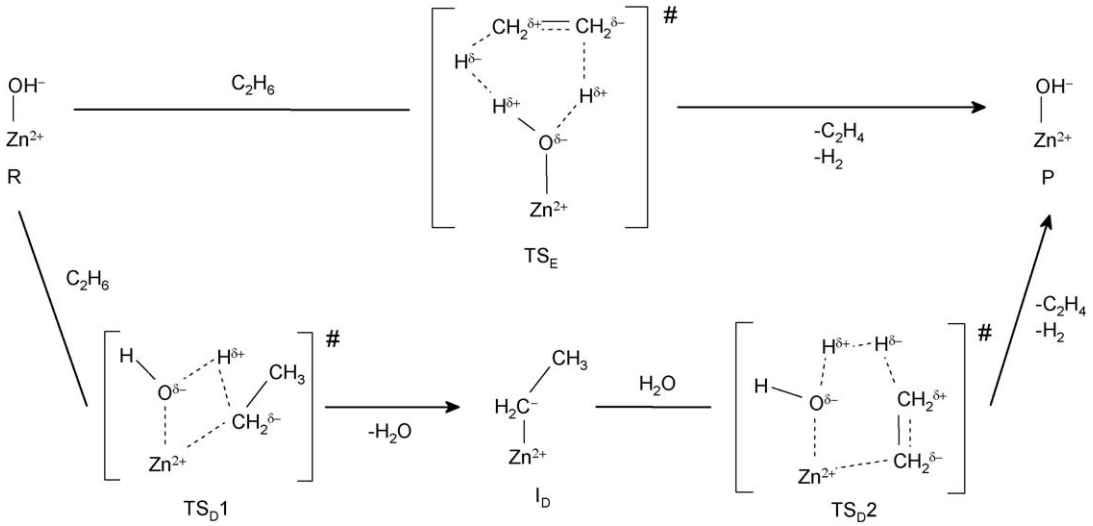

Fig. 4. Mechanisms D (lower path) and E (upper path) of ethane dehydrogenation on $ZnOH^+$ at isolated Al site.

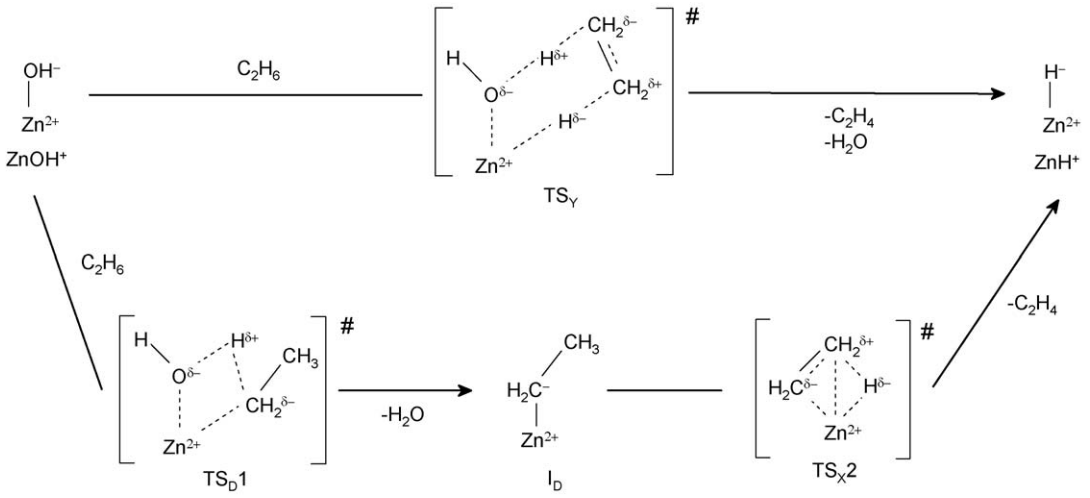

Fig. 5. Mechanisms X (lower path) and Y (upper path) of formation of new catalytic centers ZnH^+ from $ZnOH^+$ at isolated Al site.

3.4. Formation of the active center ZnH^+

The formation of ZnH^+ was modeled again by interaction of ethane with $Z1/ZnOH^+$ in two ways (Fig. 5). The first one (denoted as X) includes the same first stage as the mechanism D, where via transition state TS_D1 the intermediate $Z1/Zn(C_2H_5)^+$, I_D (Fig. 2), is formed. Then, after abstraction of ethene molecule (in absence of water) via transition state TS_X2 the new active center $Z1/ZnH^+$ (Fig. 2) is obtained. In the second mechanism (denoted as Y) two of the hydrogen atoms of ethane located at different C atoms interact respectively with the basic O center of $ZnOH^+$ and with Zn^{2+} ion. Hence via transition state TS_Y (Fig. 2) simultaneously ethene and water are released and the catalytic center $Z1/ZnH^+$ is formed. Since Zn^{2+} species is unlikely to coordinate more than one ligand [21] (in addition to the zeolite fragment), the expected intermediates $Z1/Zn(C_2H_5)(H_2O)^+$ and $Z1/Zn(H)(H_2O)^+$ were not found due to spontaneous desorption of the water molecule.

The transition state of the first stage of mechanism X has low relative enthalpy, 117 kJ/mol, while the enthalpy of the second transition state TS_X2 is significant, 254 kJ/mol (Table 2). The geometric characteristics of TS_X2 are close to those of the similar transition state TS_C (Table 1). The only significant difference is the location of $Zn(C_2H_5)^+$ moiety in TS_X2 close to the single Al center, while in TS_C it is located in the middle of the cluster.

The relative enthalpy of the transition state TS_Y is 211 kJ/mol (Table 2), i.e. significantly higher than the enthalpy of the first transition state in the mechanism X, TS_D1, however with 43 kJ/mol lower than the enthalpy of the second transition state, TS_X2.

3.5. Ethane dehydrogenation on ZnH^+ species

The interaction of ethane with ZnH^+ again is modeled via one or both methyl groups (Fig. 6). In the first case (mechanism F) heterolytic dissociation of C–H bond occurs as C atom binds to Zn^{2+} ion, while H atom interacts with the hydride anion H^- from ZnH^+, TS_F1 (Fig. 2), resulting in formation of H_2 molecule and the intermediate I_D (Fig. 2). The catalytic center ZnH^+ recovers after β-transfer of H^- from the methyl group and desorption of ethene via transition state TS_X2. In the other considered mechanism, denoted as G, the ethane molecule interacts with ZnH^+ by two of the H atoms of different CH_3 groups via TS_G (Fig. 2) and in one step C_2H_4 and H_2 are formed.

The calculated enthalpies of all transition states in mechanisms F and G are high, 221, 246, and 233 kJ/mol for TS_F1, TS_X2, and TS_G, respectively.

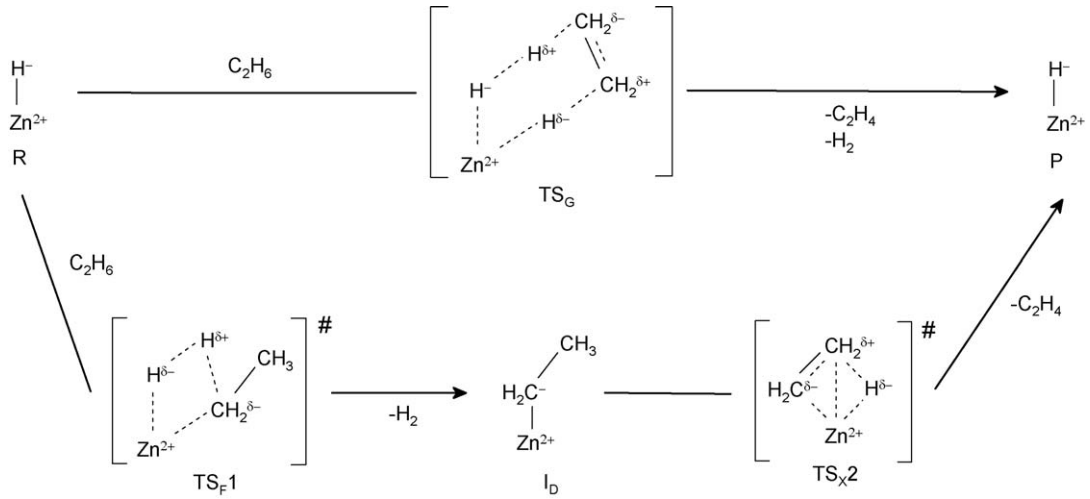

Fig. 6. Mechanisms F (lower path) and G (upper path) for ethane dehydrogenation on ZnH^+ species at isolated Al sites.

4. Discussion

4.1. Comparison of the reaction mechanisms on zinc species located at isolated and paired Al centers

4.1.1. Enthalpy

First we discuss the mechanisms of ethane dehydrogenation on the zinc species ($ZnOH^+$ and ZnH^+) located at isolated Al centers and the species (Zn^{2+}) at paired Al sites on the base of comparison between calculated relative enthalpy values for the obtained transition states with respect to corresponding reactants.

From the calculated ΔH of the transitions states on Zn^{2+} coordinated at paired Al centers we can conclude, that energetically the most favorable is the carbanionic mechanism B, where ΔH of the transition states are the lowest: 79 and 154 kJ/mol, while for the mechanism A they are 153 and 164 kJ/mol. For both mechanisms the second stages are rate-limiting. However, it should be noted that the enthalpy difference between the transition states of the two rate-limiting steps is only 9 kJ/mol.

The intermediate formed during the mechanism B, $Zn(C_2H_5)^+$, is also more stable than the corresponding intermediate of mechanism A, ZnH^+.

The enthalpies of all rate-limited transition states of the mechanisms on $ZnOH^+$ and ZnH^+ located at isolated Al centers (D–G) are above 200 kJ/mol (Table 2). Hence, we can conclude that the reaction of ethane dehydrogenation occurs much easier on Zn^{2+} species located close to paired Al centers, since the energies of the transition states in mechanisms A and B are significantly lower. It should be noted that the enthalpy of the transition state TS_D1 is relatively low, 117 kJ/mol, which supposes that interaction between ethane and $Z1/ZnOH^+$ leading to formation of the complex $Z1/Zn(C_2H_5)^+$ (denoted I_D) can occur. The ΔH value of the obtained complex $Z1/Zn(C_2H_5)^+$, located at isolated Al center, is by 27 kJ/mol lower than the value of the corresponding complex $Z2/H^+,Zn(C_2H_5)^+$ located at two Al centers, intermediate I_B. This suggests that the ethane molecule can undergo heterolytic dissociation on partially compensated zinc ions in vicinity of isolated Al center leading to formation of the complex $Zn(C_2H_5)^+$. However, ethene cannot be produced from this complex due to the high energy barrier for "intramolecular" hydride transfer from the methyl group to zinc ion via the second transition state of the mechanisms D or X, TS_D2 or TS_X2. The abstraction of a hydride ion in the complex $Z1/Zn(C_2H_5)^+$ cannot occur as "intermolecular" (as in mechanism B) since a neighboring zeolite OH group is absent due to the lack of second Al center in vicinity of the cation. The "intermolecular" process is more favorable compared to the "intramolecular" as one can estimate from the enthalpies of the corresponding transition states on zinc species at paired Al sites, TS_B2, and TS_C, 154 and 272 kJ/mol.

Theoretical investigation of other authors on the mechanism of ethane dehydrogenation on protonic form of H-ZSM-5 zeolite shows that the relative energy of the highest transition state is 288–311 kJ/mol [38–40], depending on the method and the size of the zeolite fragment. Hence, one can easily estimate that addition of Zn species in the zeolite system decreases significantly the energy of the highest transition state of alkane dehydrogenation, by more than 100 kJ/mol.

4.1.2. Gibbs free energy (influence of the entropy on the reaction mechanisms)

Since the process of ethane dehydrogenation on Zn,H-ZSM-5 zeolites occurs at high temperature, 723–823 K, [1,3,7,32] the entropy can influence significantly the preferred reaction path. By this reason we calculated Gibbs free energy of all transition states and intermediates for the considered mechanisms on the three different types of Zn species.

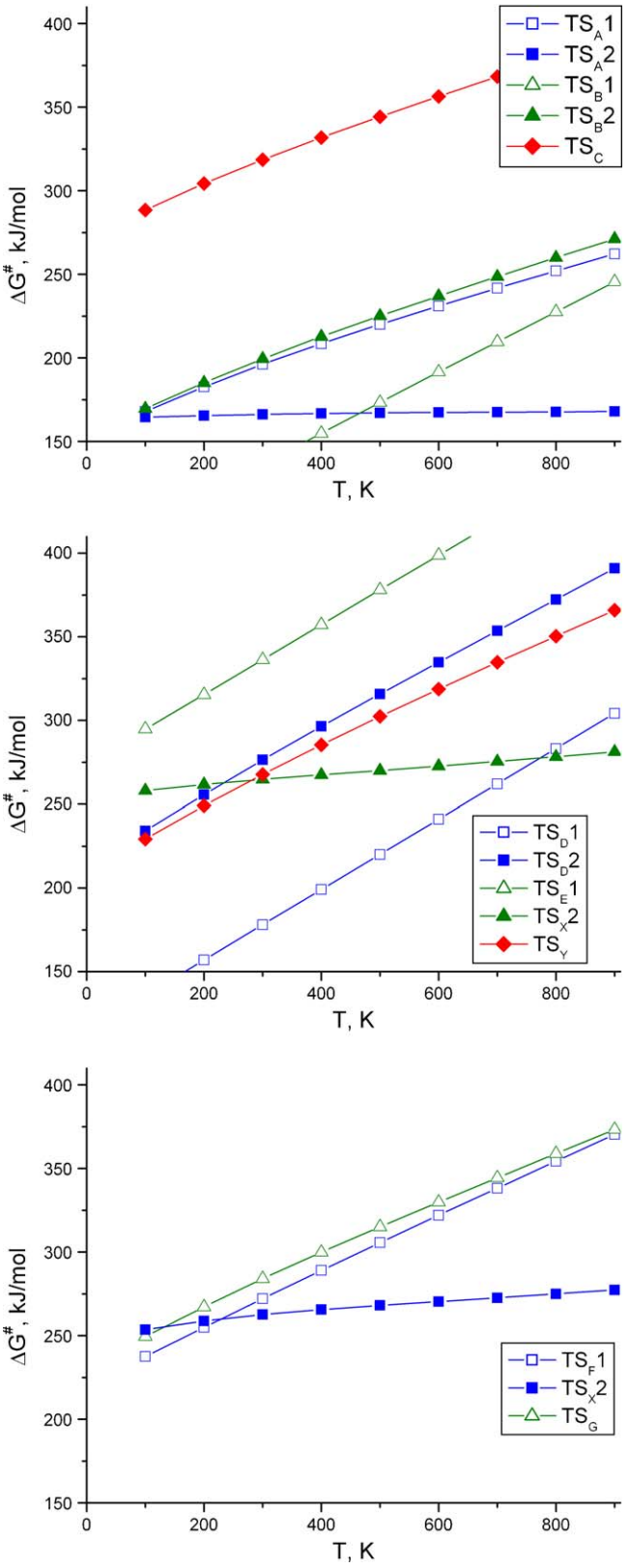

Fig. 7. Dependence of $\Delta G^{\#}$ on the reaction temperature T for all transition states included in the mechanisms of dehydrogenation on Zn^{2+} at paired Al site: A–C (upper panel); on $ZnOH^+$ at isolated Al site, D, E, X and Y (middle panel); as well as on ZnH^+ at isolated Al site, G and F (lower panel).

The values of ΔS shown in Table 2 include the contributions of all degrees of freedom for molecules in the gas phase and only vibrational degrees of freedom for the complexes in the zeolite cluster. The enthalpy and the entropy of the transition states are calculated with respect to the reactants for the corresponding mechanism. The variations of the Gibbs free energy of the corresponding transition states as function of temperature for the mechanisms A–C on $Z2/Zn^{2+}$ catalytic center are displayed in the upper panel of Fig. 7. In all cases the entropy of the initial state, $Z2/Zn^{2+}$ and ethane, is higher than the entropy of the transition states, and by this reason ΔG of the transition states increases with increasing the temperature. According to ΔG values, at temperature close to the experimental (T = 800 K) the rate-limiting stages on mechanisms A and B are the initial stage A1 and second stage B2, respectively. The entropy at T = 298 K of these transition states, TS_A1 and TS_B2, is significant −145 and −152 J/mol K (Table 2), and decrease slightly by ∼20 J/mol K with increasing the temperature to 800 K to: −124 and −132 J/mol K. Due to the significant values of the entropy with increasing the temperature, the Gibbs free energy of TS_A1 and TS_B2 increases fast (Fig. 7). At 800 K, TS_B2 has higher Gibbs free energy, 260 kJ/mol, than TS_A1, 252 kJ/mol, i.e. the mechanism A is favorable when we take into account the entropy contribution to the process. However, the energy difference at 800 K between these transition states is only 8 kJ/mol, i.e. the reaction rate of mechanism A is about three times higher than that of mechanism B. On the other hand, it should be noted that the value 8 kJ/mol is close to the limit of the accuracy of the computational method, which indicates that the reaction might occur concurrently by both mechanisms.

It is interesting that the stage with the highest entropy from both mechanisms is the recombination and desorption of hydrogen via TS_A2 with only −8 J/mol K at T = 298 K (Table 2) (the entropy slightly decreases as an absolute value to −5 J/mol K at T = 800 K), and by this reason this transition state has notably lower ΔG at high temperatures (170 kJ/mol at 800 K) than the other considered transition states. This result is in agreement with the suggestion of Biscardi et al. [1–3] based of their experimental investigations, that the catalytic role of Zn species in Zn,H-ZSM-5 zeolite during the alkane dehydrogenation is participation in the recombination and desorption of H_2, which is exactly the second stage of the mechanism A.

Similar analysis with accounting for the entropy is done also for the mechanisms of alkane dehydrogenation on the other two active centers, where zinc species are located in the vicinity of an isolated Al center. The variations of ΔG of the transition states for the mechanisms on $Z1/ZnOH^+$ (mechanisms D, E, X and Y) and on $Z1/ZnH^+$ (mechanisms F and G), as a function of temperature are displayed on the middle and lower panels of Fig. 7, respectively. The only stages which can concur with processes on the bare Zn^{2+} ions located at paired Al sites are TS_D1 and TS_X2 (283 and 278 kJ/mol at 800 K) leading to formation of $Z1/Zn(C_2H_5)^+$ or $Z1/ZnH^+$ complexes. However, the values of ΔG for continuation of the reaction on both types of intermediate complexes are by at least 100 kJ/mol higher. Thus, similarly to the conclusion based on the enthalpy values, the variation of the ΔG values again suggests that the interaction of ethane with $ZnOH^+$ or ZnH^+ species at isolated Al sites leads to formation of the intermediate $Z1/Zn(C_2H_5)^+$. In addition, from this intermediate via transition state TS_X2 $Z1/ZnH^+$ species could be formed. However, these two intermediate Zn species block the catalytic centers since the Gibbs free energies for the next reaction steps are too high.

Hence, taking into account the entropy of the system, the ΔG of the rate-limiting transition states of all mechanisms D–G are significant, above 350 kJ/mol, which is by more than 80 kJ/mol larger than the corresponding values for the mechanisms A and B of ethane dehydrogenation on Zn^{2+} at paired Al sites. This suggests that reaction of ethane dehydrogenation on Zn,H-ZSM-5 zeolite occurs (by more than 5 orders of magnitude) faster on Zn^{2+} ions located in the vicinity of two Al centers than on Zn-containing species close to isolated Al center, since on latter centers the interaction with ethane leads to formation of stable spectator species ZnH^+ or $Zn(C_2H_5)^+$, which can hardly be converted into reaction products.

One can also use the estimated ΔG values to speculate which intermediates are expected to be observed on different zinc species comparing the ΔG values of the transition states for their formation and conversion into products. On Zn^{2+} species at paired Al site the ΔG for formation of the intermediate I_A ($Z2/ZnH^+$) is always higher (above 200 K) than the corresponding value for its conversion. The difference between the two transition states at 800 K reaches 100 kJ/mol, i.e. the rate for formation of the intermediate is about 10^7 times slower than its decomposition, which suggests that intermediate ZnH^+ species at paired Al sites cannot be observed experimentally during ethane dehydrogenation. On the other hand, ΔG value for formation of the other intermediate I_B, $Z2/Zn(C_2H_5)^+$, is always lower than the values for its decomposition and this difference is highest at lower temperature. The expected ratio of the rates of the stages B1/B2 (based on the calculated ΔG values) is of the orders 10^3 and 10^4 at 800 and 500 K, respectively, i.e. $Zn(C_2H_5)^+$ species can be observed experimentally during the process at paired Al sites.

When the Zn species are close to isolated Al sites the ΔG value for formation of the intermediate I_D, $Z1/Zn(C_2H_5)^+$, is by about 100 kJ/mol (at 800 K) lower than the value for its decomposition to products via reaction path D. $Z1/Zn(C_2H_5)^+$ could be also transformed to ZnH^+ species via transition state TS_X2, due to the similar ΔG values of the steps D1 and X2. This suggests that both types of species $Zn(C_2H_5)^+$ and ZnH^+ can be observed on isolated Al sites.

4.2. Comparison with previous experimental and theoretical studies

The formation of stable species ZnH^+ or $Zn(C_2H_5)^+$ on zinc species close to isolated Al center is in good agreement with experimental study of Kazansky and Pidko [12]. They established ZnH^+ or $Zn(C_2H_5)^+$ species after reactive adsorption of H_2 or ethane, respectively, on Zn,H-ZSM-5 zeolites, obtained by exchange of H-ZSM-5 zeolite with Zn vapors that presumably contain partially compensated Zn^{2+} cations. For $Zn(C_2H_5)^+$ they detected several characteristic IR bands at 2874, 2910, 2958 and a shoulder about 2980 cm^{-1} (see Fig. 6 in Ref. [12]), which were assigned to the C–H stretching modes. Indeed, we calculated similar values of the C–H frequencies in the intermediate I_D representing the structure $Z1/Zn(C_2H_5)^+$: 2880, 2905, 2942, 2948 and 2979 cm^{-1} (see note [41]). However, the C–H frequencies of the same species located in vicinity of paired Al cites as in the intermediate I_B: 2877, 2913, 2941, 2952 and 2975 cm^{-1}, are also in good agreement with the experimental values. In the experiment, above 500 K the $Zn(C_2H_5)^+$ species are transformed into ZnH^+ species characterized by an IR vibrational frequency of 1934 cm^{-1} [10,42].

Stable $Zn(CH_3)^+$ species were also detected recently by MAS NMR [14] when methane is adsorbed on Zn,H-ZSM-5 zeolites, obtained by exchange of H-ZSM-5 zeolite with Zn vapors. The experiments showed that $Zn(CH_3)^+$ species can be observed at ambient temperature only on Zn species close to isolated Al centers, while on Zn^{2+} close to Al pairs such species are not detected. This conclusion is in agreement with the higher stability of the ZnR^+ species at isolated than at the paired Al sites obtained in the present work. Along the line of our discussion for ethane dissociation on zinc sites, methane dissociation on Zn^{2+} at paired Al sites results in formation of $Zn(CH_3)^+$ and a neighboring bridging OH group that allows easy recombination and desorption of

methane. On the other hand, on zinc species at isolated Al centers methane dissociation creates a distant OH group at the second Al center (that formally balances the charge of the partially compensated Zn^{2+} ion in the sample). By this reason the recombination of methane is rather difficult and $Zn(CH_3)^+$ species have long live-time, sufficient to be detected by MAS NMR measurement.

As it was mentioned in the Introduction, the mechanisms B and C, occurring via carbanionic intermediate I_B, have been already modeled computationally in several studies using density functional method with B3LYP functional [26–29]. The former study [26] was based on four-membered zeolite ring models, while the latter ones on 2 five-membered rings [27–29]. The geometrical parameters of most of the structures, obtained in present study and in Refs. [27–29], are similar. The deviations are within 5 pm at most although different zeolite models are used. The only exception is TS_B2 structure, where the O_z–H distance in our structure, 157 pm, is larger by 13 pm than the distance in the structure obtained in Ref. [29], 145 pm. The calculated energy values reported by Pidko and van Santen [29] are by 42, 30, and 71 kJ/mol higher for the transition states TS_A2, TS_B1, and TS_B2 with respect to the corresponding values obtained in our study. In the latter case the larger energy difference could be related to the different models, more flexible basis set used in the present study (6-311+G** here versus combination of 6-31G**, 6-311G**, and D95 in Ref. [29]) and the larger elongation of the O–H distance mentioned above. On the other hand, the calculated energy for the TS_C reported by Pidko and van Santen [29], 262 kJ/mol, is lower by 10 kJ/mol than the result in the present study, 272 kJ/mol.

Summarizing the results of the previous theoretical and experimental studies one can conclude that depending on the preparation technique of Zn,H-ZSM-5 zeolites, different Zn species could be formed and could act as catalysts for the alkane dehydrogenation.

When Zn,H-ZSM-5 zeolites is prepared by ion exchange from water solution of zinc salt [2] two types of Zn species should exist in the pores of ZSM-5 zeolite: $ZnOH^+$ at isolated Al center and at two closely located Al centers (e.g. Al pair) – Zn^{2+}, formed from $Zn(H_2O)^{2+}$ after desorption of water at high temperature. Our present calculations showed that ethane dehydrogenation can occur significantly easier on the latter species.

When Zn,H-ZSM-5 zeolites is prepared by exchange of H-ZSM-5 zeolite with Zn vapors two types of Zn^{2+} cations are suggested to exist: (1) Zn^{2+} in vicinity of isolated Al center and (2) Zn^{2+} in vicinity of two Al centers. According to the calculations of Pidko and van Santen [29], who modeled the mechanisms denoted here as B and C on both types of Zn^{2+} ions (located close to one or two Al centers), the dehydrogenation reaction would occur with lowest activation barrier on Zn^{2+} located close to only one Al center via mechanism B with the apparent activation energy of only 153 kJ/mol and an energy barrier of the rate-limiting reaction step B2 of 147 kJ/mol. Due to the lack of second Al center in the ring with the Zn^{2+} cation, the intermediate, formed along this reaction pathway, contains $Zn(C_2H_5)^+$ species and Si–O(H)–Si hydroxyl group, while the second Al center in the neighboring five-membered ring remains uncompensated. According to Shubin et al. [28], the proton from Si–O(H)–Si hydroxyl group could easily migrate towards the distant Al center (with a reaction barrier of only 59 kJ/mol) that will result in the most stable intermediate with a distant Al–O(H)–Si group. Since in the obtained structure both Al centers are charge compensated, this intermediate is more stable by 129 kJ/mol than initial structure with Si–O(H)–Si fragment [28], i.e. the proton can hardly be returned back to the Si–O(H)–Si bridge due to the high energy barrier for the reverse transfer, 188 kJ/mol [28]. By this reason, on Zn^{2+} species at isolated Al sites the dehydrogenation reaction would stop since the OH group in vicinity of the $Zn(C_2H_5)^+$ species is not available, in complete agreement with the conclusions from our model calculations.

When Zn,H-ZSM-5 zeolite is prepared by incipient wetness impregnation, in addition to the Zn^{2+} and $ZnOH^+$, external ZnO crystallites [2], as well as $ZnOZn^{2+}$ species could exist [15–19]. Pidko and van Santen [29] modeled dehydrogenation on $ZnOZn^{2+}$ and showed that heterolytic C_2H_6 dissociation results in formation of very stable species: $ZnOH^+$ and $Zn(C_2H_5)^+$, and according to the authors, formation of ethene afterwards is kinetically and thermodynamically unfavored. However, Stepanov et al. [17] proposed another mechanism of dehydrogenation which includes simultaneously not only $ZnOZn^{2+}$ but also zeolite acidic site Si–OH–Al and supposed synergism between Zn species and a neighboring bridging OH group of the zeolite.

5. Conclusions

Our computational model study of the ethane dehydrogenation on the active sites in Zn,H-ZSM-5 zeolite prepared by ion exchange suggests that the reaction occurs faster on Zn^{2+} ions located in the vicinity of two Al centers, while on Zn species close to isolated Al center, stable spectator species ZnH^+ or $Zn(C_2H_5)^+$ are formed. However, further catalytic reaction on these species does not occur due to the high energetic barriers on the next stages of the dehydrogenation process. This conclusion highlights the crucial role of the second Al center in vicinity of the zinc ion for ethane dehydrogenation:

- in synchronic mechanism A the presence of second Al center ensure basic O center at appropriate distance, which can interact with one of the H atoms of the ethane;
- in the dissociative mechanism B, the second Al center ensure not only basic O center for initial cleavage of C–H bond, but also bridging OH group, which interacts with ethanide anion in the second stage.

On the catalytic centers Zn^{2+}, the reaction occurs concurrently on both A and B mechanisms with rate-limiting stages, respectively: A1 – synchronic abstraction of H^- and H^+ from the ethane, and B2 – abstraction of a H^- from the ethanide anion and formation of the reaction products.

Acknowledgments

The work was supported by the National Center of Advanced Materials UNION and the contract D002-184/08 with Bulgarian National Science Fund.

References

[1] J.A. Biscardi, E. Iglesia, J. Catal. 182 (1999) 117.
[2] J.A. Biscardi, G.D. Meitzner, E. Iglesia, J. Catal. 179 (1998) 192.
[3] S.Y. Yu, J.A. Biscardi, E. Iglesia, J. Phys. Chem. B 106 (2002) 9642.
[4] A. Hagen, E. Schneider, M. Benter, A. Krogh, A. Kleinert, F. Roessner, J. Catal. 226 (2004) 171.
[5] J. Heemsoth, E. Tegeler, F. Roessner, A. Hagen, Micropor. Mesopor. Mater. 46 (2001) 185.
[6] A. Smieskova, E. Rojasova, P. Hudec, L. Sabo, React. Kinet. Catal. Lett. 82 (2004) 227.
[7] H. Berndt, G. Lietz, B. Lücke, J. Völter, Appl. Catal. A: Gen. 146 (1996) 351.
[8] Y. Sun, T.C. Brown, Int. J. Chem. Kinet. 34 (2002) 467.
[9] H. Berndt, G. Lietz, J. Völter, Appl. Catal. A: Gen. 146 (1996) 365.
[10] V.B. Kazansky, A.I. Serykh, Phys. Chem. Chem. Phys. 6 (2004) 3760.
[11] E.M. El-Malki, R.A. van Santen, W.M.H. Sachtler, J. Phys. Chem. B 103 (1999) 4611.
[12] V.B. Kazansky, E.A. Pidko, J. Phys. Chem. B 109 (2005) 2103.
[13] V.B. Kazansky, J. Catal. 216 (2003) 192.
[14] Y.G. Kolyagin, I.I. Ivanova, V.V. Ordomsky, A. Gedeon, Y.A. Pirogov, J. Phys. Chem. C 112 (2008) 20065.
[15] Y.G. Kolyagin, V.V. Ordomsky, Y.Z. Khimyak, A.I. Rebrov, F. Fajula, I.I. Ivanova, J. Catal. 238 (2006) 122.
[16] A.G. Stepanov, S.S. Arzumanov, V.N. Parmon, Yu.G. Kolyagin, I.I. Ivanova, D. Freude, Catal. Lett. 114 (2007) 85.

[17] A.G. Stepanov, S.S. Arzumanov, A.A. Gabrienko, V.N. Parmon, I.I. Ivanova, D. Freude, Chem. Phys. Chem. 9 (2008) 2559.
[18] M.V. Luzgin, V.A. Rogov, S.S. Arzumanov, A.V. Toktarev, A.G. Stepanov, V.N. Parmon, Angew. Chem. Int. Ed. 47 (2008) 4559.
[19] A.G. Stepanov, S.S. Arzumanov, A.A. Gabrienko, A.V. Toktarev, V.N. Parmon, D. Freude, J. Catal. 253 (2008) 11.
[20] H.A. Aleksandrov, G.N. Vayssilov, N. Rösch, Stud. Surf. Sci. Catal. 158 (2005) 593.
[21] H.A. Aleksandrov, Ph.D. Thesis, University of Sofia, Sofia, 2008.
[22] G.N. Vayssilov, H.A. Aleksandrov, G.P. Petrova, P.St. Petkov, in: V. Valchev, S. Mintova, M. Tsapatsis (Eds.), Ordered Porous Solids, Elsevier, Amsterdam, 2008, p. 209.
[23] H.A. Aleksandrov, G.N. Vayssilov, N. Rösch, J. Molec. Catal. A: Chem. 256 (2006) 149.
[24] M.J. Rice, A.K. Chakraborty, A.T. Bell, J. Phys. Chem. B 104 (2000) 9987.
[25] A.T. Bell, in: G. Centi, B. Wichterlowa, A.T. Bell (Eds.), Catalysis by Unique Metal Ion Structures in Solid Matrixes, Kluwer Academic Publishers, Dordrecht, 2000 p. 55.
[26] M.V. Frash, R.A. van Santen, Phys. Chem. Chem. Phys. 2 (2000) 1085.
[27] G.M. Zhidomirov, A.A. Shubin, V.B. Kazansky, R.A. van Santen, Theor. Chem. Acc. 114 (2005) 90.
[28] A.A. Shubin, G.M. Zhidomirov, V.B. Kazansky, R.A. van Santen, Catal. Lett. 90 (2003) 137.
[29] E.A. Pidko, R.A. van Santen, J. Phys. Chem. C 111 (2007) 2643.
[30] N.A. Kachurovskaya, G.M. Zhidomirov, R.A. van Santen, Res. Chem. Intermed. 30 (2004) 99.
[31] L. Benco, T. Bucko, J. Hafner, H. Toulhoat, J. Phys. Chem. B 109 (2005) 20361.
[32] J.A. Biscardi, E. Iglesia, Phys. Chem. Chem. Phys. 1 (1999) 5753.
[33] (a) J. Gale, GULP, 1.3 version, Imperial College, London, 2002.
(b) J.D. Gale, J. Chem. Soc. Faraday Trans. 93 (1997) 629.
[34] V.A. Nasluzov, E.A. Ivanova, A.M. Shor, G.N. Vayssilov, U. Birkenheuer, N. Rösch, J. Phys. Chem. B 107 (2003) 2228.
[35] E.A. Ivanova Shor, A.M. Shor, V.A. Nasluzov, G.N. Vayssilov, N. Rösch, J. Chem. Theory Comp. 1 (2005) 459.
[36] M.J. Frisch, G.W. Trucks, H.B. Schlegel, G.E. Scuseria, M.A. Robb, J.R. Cheeseman, J.A. Montgomery Jr., T. Vreven, K.N. Kudin, J.C. Burant, J.M. Millam, S.S. Iyengar, J. Tomasi, V. Barone, B. Mennucci, M. Cossi, G. Scalmani, N. Rega, G.A. Petersson, H. Nakatsuji, M. Hada, M. Ehara, K. Toyota, R. Fukuda, J. Hasegawa, M. Ishida, T. Nakajima, Y. Honda, O. Kitao, H. Nakai, M. Klene, X. Li, J.E. Knox, H.P. Hratchian, J.B. Cross, V. Bakken, C. Adamo, J. Jaramillo, R. Gomperts, R.E. Stratmann, O. Yazyev, A.J. Austin, R. Cammi, C. Pomelli, J.W. Ochterski, P.Y. Ayala, K. Morokuma, G.A. Voth, P. Salvador, J.J. Dannenberg, V.G. Zakrzewski, S. Dapprich, A.D. Daniels, M.C. Strain, O. Farkas, D.K. Malick, A.D. Rabuck, K. Raghavachari, J.B. Foresman, J.V. Ortiz, Q. Cui, A.G. Baboul, S. Clifford, J. Cioslowski, B.B. Stefanov, G. Liu, A. Liashenko, P. Piskorz, I. Komaromi, R.L. Martin, D.J. Fox, T. Keith, M.A. Al-Laham, C.Y. Peng, A. Nanayakkara, M. Challacombe, P.M.W. Gill, B. Johnson, W. Chen, M.W. Wong, C. Gonzalez, J.A. Pople, Gaussian 03, Revision B.05, Gaussian, Inc., Pittsburgh, PA, 2003.
[37] (a) A.D. Becke, Phys. Rev. A 38 (1988) 3098;
(b) J.P. Perdew, Phys. Rev. B 33 (1986) 8822;
J.P. Perdew, Phys. Rev. B 34 (1986) 7406.
[38] S. Senger, L. Radom, J. Am. Chem. Soc. 122 (2000) 2613.
[39] S.R. Blaszkowski, M.A.C. Nascimento, R.A. van Santen, J. Phys. Chem. 100 (1996) 3463.
[40] E.A. Furtado, I. Milas, J.O.M.D.A. Lins, M.A.C. Nascimento, Phys. Stat. Sol. 187 (2001) 275.
[41] Calculated C–H frequencies of the ethane molecule in gas phase differ from the experimental values by -49 ± 8 cm^{-1}. By this reason all calculated C–H frequencies in the intermediates I_B and I_D are corrected with -49 cm^{-1}.
[42] V.B. Kazansky, A.I. Serikh, B.G. Anderson, R.A. van Santen, Catal. Lett. 88 (2003) 211.